An iterative thresholding algorithm for the neuronal current imaging

Gabriella Bretti, Francesca Pitolli *

Dip. Me.Mo.Mat., Università di Roma "La Sapienza"

Via A. Scarpa 16, 00161 Roma, Italy

Abstract

Neuronal current imaging aims at analyzing the functionality of the human brain through the localization of those regions where the neural current flows. The reconstruction of an electric current distribution from its magnetic field measured in the outer space, gives rise to a highly ill-posed and ill-conditioned inverse problem. We use a joint sparsity constraint as a regularization term and we propose an efficient iterative thresholding algorithm to reconstruct the current distribution. Some numerical tests are also displayed.

Keywords: Electric current imaging, Magnetoencephalograpy, Inverse problem, Sparsity constraint, Iterative thresholding, Multiscale basis.

1 Introduction

Bioelectric current imaging aims at analyzing the functionality of the human internal organs through the localization of those regions where their electric activity arises. In particular, magnetoencephalographic (MEG) neuroimaging aims at detecting the brain active regions through the measurements of the tiny magnetic field generated outside the brain by neuronal currents (see [4], and references therein).

* *E-mail address:* {bretti,pitolli}@dmmm.uniroma1.it

Since the neuromagnetic field can be very weak and affected by high noise, the measurements are performed by very sensitive magnetometers based on Superconducting QUantum Interference Devices (SQUIDs). Nevertheless, a sophisticated data analysis is needed.

MEG measurements do not directly provide a neuronal current image and we need a model linking the current distribution to the external magnetic field. Actually, electric current imaging requires to solve a linear inverse problem which usually do not have a unique solution [7, 12] so that further constraints on the solution have to be added. Regularization techniques which use a quadratic constraint, give good results when the quantities under observation are equally distributed in time or space [7]. However, the current distribution we want to reconstruct can be often represented as a sum of weighted basic currents with only few significant terms, i.e. it has a *sparse representation* [5]. To promote sparsity in the reconstruction of scalar quantities, a regularization technique based on *non quadratic constraints* was introduced in [3] and the solution of the inverse problem was approximated by a convergent thresholded Landweber algorithm. A generalization to the vector case by means of a *joint sparsity constraint* was proposed in [9] and joint sparsity was used in [8] to regularized the MEG inverse problem. Following [10], in this paper we introduce an efficient algorithm to numerically solve the MEG inverse problem and we show that the resulting thresholded iteration is convergent. Numerical tests show that joint sparsity outperforms Tikhonov regularization and soft thresholding [6], especially when the data are affected by high noise.
The paper is organized as follows. The inverse MEG problem is briefly recalled in Section 2. Then, in Section 3 we introduce the joint sparsity constraint as a regularization term. A convergent iterative thresholding algorithm which solves the MEG inverse problem is outlined in Section 4. Finally, some numerical tests are displayed in Section 5.

2 The MEG Inverse Problem

Let us model the head as a set of different regions, say V_k, $k = 0, \ldots, K$, with constant conductivity σ_k, such that

$$V_k \subset V_{k+1}, \qquad k = 0, \ldots, K-1. \tag{1}$$

The regions V_k, $k = 0, \ldots, K-1$, represent different anatomical parts, i.e. the brain, the cerebrospinal fluid, the meninges, the skull, etc. The neuronal currents $\vec{\mathbf{J}}$ are confined to the brain, represented by the innermost region V_0. The external magnetic field $\vec{\mathbf{B}}$ is linked to the current $\vec{\mathbf{J}}$ by the *Biot-Savart law* [12]

$$\begin{aligned} \vec{\mathbf{B}}(\vec{\mathbf{r}}) &= \vec{\mathbf{B}}_\infty(\vec{\mathbf{r}}) - \\ &- \frac{\mu_0}{4\pi} \sum_{k=0}^{K} (\sigma_{k+1} - \sigma_k) \int_{\partial V_k} \frac{\Phi(\vec{\mathbf{r}}')\, \vec{\mathbf{e}}_k(\vec{\mathbf{r}}') \times (\vec{\mathbf{r}} - \vec{\mathbf{r}}')}{|\vec{\mathbf{r}} - \vec{\mathbf{r}}'|^3} \, d\big(\partial V_k(\vec{\mathbf{r}}')\big) \,, \end{aligned} \tag{2}$$

where $\mathbf{B}_\infty$ is the magnetic field in an infinite homogeneous medium with magnetic permeability μ_0, i.e.

$$\vec{\mathbf{B}}_\infty(\vec{\mathbf{r}}) = \frac{\mu_0}{4\pi} \int_{V_0} \vec{\mathbf{J}}(\vec{\mathbf{r}}') \times \frac{\vec{\mathbf{r}} - \vec{\mathbf{r}}'}{|\vec{\mathbf{r}} - \vec{\mathbf{r}}'|^3} \, d\vec{\mathbf{r}}' \,, \tag{3}$$

Φ is the electric potential on the surfaces ∂V_k and $\vec{\mathbf{e}}_k$ is the unit normal w.r.t. ∂V_k, the surface between V_k and V_{k+1}. Note that σ_{K+1} is set equal to 0.

Let $\vec{\mathbf{q}}_l$, $l = 1, \ldots, N$, be the site coordinates of the magnetometers, which are located on a spherical surface Ω centered at the origin with $\delta := dist(V_K, \partial\Omega) > 0$. Usually, just the normal component w.r.t. to Ω is measured, i.e.

$$B_r(\vec{\mathbf{q}}_l) := \vec{\mathbf{B}}(\vec{\mathbf{q}}_l) \cdot \vec{\mathbf{e}}_r(\vec{\mathbf{q}}_l), \quad l = 1, \ldots, N, \tag{4}$$

where $\vec{\mathbf{e}}_r(\vec{\mathbf{q}}_l)$ is the unit normal w.r.t. to Ω in $\vec{\mathbf{q}}_l$.

Here, we assume that the regions V_k are concentric spheres of increasing radius and centered at the origin. Then, recalling that for any three vectors in $\mathbf{R}^3$ it holds $v \times w \cdot z = -z \times w \cdot v$, one has:

$$\mathcal{B}(\vec{\mathbf{J}}, \vec{\mathbf{q}}_l) := B_r(\vec{\mathbf{q}}_l) = \frac{\mu_0}{4\pi} \int_{V_0} \frac{\vec{\mathbf{e}}_r(\vec{\mathbf{q}}_l) \times (\vec{\mathbf{q}}_l - \vec{\mathbf{r}}')}{|\vec{\mathbf{q}}_l - \vec{\mathbf{r}}'|^3} \cdot \vec{\mathbf{J}}(\vec{\mathbf{r}}') \, d\vec{\mathbf{r}}' \,. \tag{5}$$

We remark that, due to the spherical symmetry, the magnetic field generated by the electric potential do not contribute to B_r.

The normal component of $\vec{\mathbf{B}}$ on a surface external to the brain uniquely determines the magnetic field out of the head as soon as the current flux on the scalp is known. In fact, this is the case since the current flux is null.

The MEG inverse problem aims at reconstructing the current distribution $\vec{\mathbf{J}}$ starting from the normal component of the magnetic field measured in

$\vec{\mathbf{q}}_l$. In order to identify the current sources from the measurements $\mathbf{M} = (m_1, \ldots, m_N)$ we have to minimize the discrepancy

$$\Delta(\vec{\mathbf{J}}) := \left\| \mathbf{G}(\vec{\mathbf{J}}) - \mathbf{M} \right\|_{\mathbf{R}^N}^2 , \tag{6}$$

where $\mathbf{G}(\vec{\mathbf{J}}) = \big(\mathcal{B}(\vec{\mathbf{J}}, \vec{\mathbf{q}}_1), ..., \mathcal{B}(\vec{\mathbf{J}}, \vec{\mathbf{q}}_N)\big)$.

Unfortunately, this is a strongly ill-posed problem since there exist silent currents that do not produce any magnetic field in the outer space, so that non unique solutions can be expected. For these reasons the minimization of the discrepancy might not be feasible and some regularization technique is required.

3 A Joint Sparsity Constraint for the MEG Inverse Problem

Let us assume that the current density $\vec{\mathbf{J}} = (J_1, J_2, J_3) \in L_2(V_0; \mathbf{R}^3)$ can be *sparsely* represented by a suitable dictionary $\mathcal{D} := (\psi_\lambda)_{\lambda \in \mathbf{\Lambda}}$, i.e.

$$J_\ell \approx \sum_{\lambda \in \mathbf{\Lambda}_S} j_\lambda^\ell \, \psi_\lambda \, , \qquad j_\lambda^\ell = \langle J_\ell, \psi_\lambda \rangle \, , \qquad \ell = 1, 2, 3, \tag{7}$$

where $\mathbf{\Lambda}_S \subset \mathbf{\Lambda}$ is the set of the *few* significant coefficients j_λ^ℓ [5]. As a dictionary we choose a stable multiscale basis $(\psi_\lambda)_{\lambda \in \mathbf{\Lambda}} \in L_2(V_0, \mathbf{R})$, for instance, a wavelet basis [2] or a frame system [1].

By using the decomposition (7), the discrepancy (6) can be written as

$$\Delta(\vec{\mathbf{j}}) = \left\| T \vec{\mathbf{j}} - \mathbf{M} \right\|_{\mathbf{R}^N}^2 , \tag{8}$$

where $\vec{\mathbf{j}} := (j_\lambda^\ell)_{\lambda \in \Lambda, \ell = 1,2,3}$ and the operator $T : \ell_2(\Lambda, \mathbf{R}^3) \to \mathbf{R}^N$ has entries given by

$$(T \vec{\mathbf{j}})_l \;\; = \;\; \sum_{\ell=1}^{3} \sum_{\lambda \in \mathbf{\Lambda}} j_\lambda^\ell \, \frac{\mu_0}{4\pi} \int_{V_0} \left(\frac{\vec{\mathbf{e}}_z(\vec{\mathbf{q}}_l) \times (\vec{\mathbf{q}}_l - \vec{\mathbf{r}}\,')}{|\vec{\mathbf{q}}_l - \vec{\mathbf{r}}\,'|^3} \right)_\ell \psi_\lambda(\vec{\mathbf{r}}\,') \, d\vec{\mathbf{r}}\,'. \tag{9}$$

Thus, the MEG inverse problem can be set as follows.

Given a set of magnetic field measurements $\mathbf{M}$*, determine the decomposition coefficients* $\vec{\mathbf{j}}$ *that minimize the functional*

$$\mathcal{J}_{\mathbf{\Psi}}(\vec{\mathbf{j}}) := \mathbf{\Delta}(\vec{\mathbf{j}}) + \mathbf{\Psi}_{\mathcal{D}}(\vec{\mathbf{j}}), \tag{10}$$

where $\mathcal{D}$ *is a dictionary chosen in order the solution of the minimum problem is sparsely represented, and* $\mathbf{\Psi}_{\mathcal{D}}$ *is the* joint sparsity measure

$$\mathbf{\Psi}_{\mathcal{D}}(\vec{\mathbf{j}}, v) := \sum_{\lambda\in\mathbf{\Lambda}} v_\lambda \, \|\vec{\mathbf{j}}_\lambda\|_p + \sum_{\lambda\in\mathbf{\Lambda}} \omega_\lambda \|\vec{\mathbf{j}}_\lambda\|_2^2 + \sum_{\lambda\in\mathbf{\Lambda}} \theta_\lambda (\rho_\lambda - v_\lambda)^2, \quad p \geq 1. \tag{11}$$

introduced in [9].

Here, $(\theta_\lambda)_{\lambda\in\mathbf{\Lambda}}$, $(\rho_\lambda)_{\lambda\in\mathbf{\Lambda}}$, $(\omega_\lambda)_{\lambda\in\mathbf{\Lambda}}$ are positive sequences and $\|\cdot\|_p$ denotes the usual p-norm for vectors in $\mathbf{R}^3$.

Thus, the MEG inverse problem with the joint sparsity constraint consists in minimizing the functional

$$\mathcal{J}^{(p)}_{\theta,\omega,\rho}(\vec{\mathbf{j}}, v) = \sum_{l=1}^{N} \left| (T\vec{\mathbf{j}})_l - m_l \right|^2 + \sum_{\lambda\in\mathbf{\Lambda}} v_\lambda \, \|\vec{\mathbf{j}}_\lambda\|_p + \sum_{\lambda\in\mathbf{\Lambda}} \omega_\lambda \|\vec{\mathbf{j}}_\lambda\|_2^2 + \sum_{\lambda\in\mathbf{\Lambda}} \theta_\lambda (\rho_\lambda - v_\lambda)^2 \tag{12}$$

jointly with respect to both $\vec{\mathbf{j}}$ and v, restricted to $v_\lambda \geq 0$.

The minimization of $\mathcal{J}^{(p)}_{\theta,\omega,\rho}$ promotes that all entries of the vector $\vec{\mathbf{j}}_\lambda$ have the *same sparsity* pattern. Note that v serves as an indicator of large values of $\|\vec{\mathbf{j}}_\lambda\|_p$ and $0 \leq v_\lambda \leq \rho_\lambda$, $\lambda \in \mathbf{\Lambda}$, at the minimum. The quadratic term $\sum_{\lambda\in\mathbf{\Lambda}} \omega_\lambda \|\vec{\mathbf{j}}_\lambda\|_2^2$ makes the overall functional convex, depending on a suitable choice of the sequence $(\omega_\lambda)_{\lambda\in\mathbf{\Lambda}}$ (see [9] for details).

We remark that when $\theta_\lambda = 0$ and $\omega_\lambda = \alpha$ (a fixed constant) for all $\lambda \in \Lambda$, we obtain the usual Tikhonov regularization since $(v_\lambda)_{\lambda\in\Lambda} = 0$ in this case.

4 An Iterative Thresholding Algorithm for the MEG Inverse Problem

The minimizer $(\vec{\mathbf{j}}^*, v^*)$ of the functional $\mathcal{J}^{(p)}_{\theta,\rho,\omega}$ can be approximated by the following iterative thresholding algorithm deduced from [10].

Algorithm JS

$$
\left\{
\begin{array}{l}
\textit{Let } \gamma \textit{ be a suitable relaxation parameter} \\
\\
\textit{Choose the positive sequences } \quad (\theta_\lambda)_{\lambda\in\mathbf{\Lambda}},\ (\rho_\lambda)_{\lambda\in\mathbf{\Lambda}},\ (\omega_\lambda)_{\lambda\in\mathbf{\Lambda}} \\
\\
\textit{Choose } \quad \vec{\mathbf{j}}^{(0)} = 0 \\
\\
\textit{For } \quad 0 \le k \le K \quad \textit{do} \\
\\
\qquad \textit{Let } \quad \nu_\lambda^{(0)} = \rho_\lambda \textit{ and } \quad \vec{\mathbf{z}}_\lambda^{(0)} = \vec{\mathbf{j}}_\lambda^{(k)} + \gamma \left(T^*(M - T\,\vec{\mathbf{j}}^{(k)})\right)_\lambda \quad \lambda \in \mathbf{\Lambda} \\
\\
\qquad \textit{For } \quad 0 \le r \le R \quad \textit{do} \\
\\
\qquad\qquad \vec{\mathbf{z}}_\lambda^{(r+1)} = S^{(p)}_{\nu_\lambda^{(r)}}\left(\vec{\mathbf{z}}_\lambda\right) \quad \lambda \in \Lambda \\
\\
\qquad\qquad \nu_\lambda^{(r+1)} = \left\{ \begin{array}{ll} \rho_\lambda - \frac{1}{2\theta_\lambda(1+\omega_\lambda)}\|\vec{\mathbf{z}}_\lambda^{(r+1)}\|_p & \textit{if } \|\vec{\mathbf{z}}_\lambda^{(r+1)}\|_p < 2\theta_\lambda(1+\omega_\lambda)\rho_\lambda \\ 0 & \textit{otherwise} \end{array} \right. \quad \lambda \in \mathbf{\Lambda} \\
\\
\textit{Approximate } \quad \vec{\mathbf{j}}_\lambda^{(k+1)} \approx \dfrac{\vec{\mathbf{z}}_\lambda^{(R+1)}}{1+\omega_\lambda} \qquad \lambda \in \mathbf{\Lambda} \\
\\
\textit{Compute } \quad v_\lambda^{(K+1)} = \left\{ \begin{array}{ll} \rho_\lambda - \frac{1}{2\theta_\lambda}\|\vec{\mathbf{j}}_\lambda^{(K+1)}\|_p & \textit{if } \|\vec{\mathbf{j}}_\lambda^{(K+1)}\|_p < 2\theta_\lambda\rho_\lambda \\ 0 & \textit{otherwise} \end{array} \right. \qquad \lambda \in \mathbf{\Lambda}
\end{array}
\right.
$$

We remark that, usually, the values $(v_\lambda^{(K+1)})_{\lambda\in\mathbf{\Lambda}}$ are not needed.

The operator $S_\nu^{(p)}(\vec{\mathbf{z}}) = \left(S_\nu^{(p)}(\vec{\mathbf{z}})\right)_{\ell=1,2,3}$ is a thresholding operator whose explicit expression for $p = 1, 2$ is (cf. [9]):

$$
\left(S_\nu^{(1)}(\vec{\mathbf{z}})\right)_\ell = s_\nu^{(1)}(z_\ell) := \left\{ \begin{array}{ll} z_\ell - sign(z_\ell)\frac{\nu}{2} & \text{if} \quad |z_\ell| > \frac{\nu}{2}, \\ \\ 0 & \text{otherwise,} \end{array} \right. \tag{13}
$$

$$S_\nu^{(2)}(\vec{\mathbf{z}}) := \begin{cases} \frac{\|\vec{\mathbf{z}}\|_2 - \nu/2}{\|\vec{\mathbf{z}}\|_2}\,\vec{\mathbf{z}} & \text{if} \quad \|\vec{\mathbf{z}}\|_2 > \frac{\nu}{2}, \\ \\ 0 & \text{otherwise.} \end{cases} \tag{14}$$

Theorem 4.1. *Let $p = 1, 2, \infty$, and assume*

$$\inf_{\lambda\in\mathbf{\Lambda}} \theta_\lambda(s_{\min} + \omega_\lambda) > \frac{\kappa_p}{4}, \tag{15}$$

where $s_{\min}$ is the minimum of the spectrum of T^*T, and κ_p is a constant whose value is 3 for $p = 1$ and 1 for $p = 2, \infty$. Then, the Algorithm JS converges strongly to the unique couple $(\vec{\mathbf{j}}^*, v^*)$ minimizing the functional $\mathcal{J}^{(p)}_{\theta,\rho,\omega}$. Moreover, we have the error estimate

$$\|\vec{\mathbf{j}}^{(k)} - \vec{\mathbf{j}}^*\|_2 \le \beta^k \, \|\vec{\mathbf{j}}^{(0)} - \vec{\mathbf{j}}^*\|_2, \tag{16}$$

where $\beta := \sup_{\lambda\in\mathbf{\Lambda}} \frac{4\theta_\lambda(1-s_{\min})}{4\theta_\lambda(1+\omega_\lambda)-\kappa_p} < 1$.

Proof. From [10, Lemma 2.1] it follows that $\mathcal{J}^{(p)}_{\theta,\rho,\omega}$ is strictly convex and has a unique minimizer. Then, the claim follows from Prop. 3.4 and Th. 4.3 in [10]. □

In order to implement the algorithm we need to evaluate $T^*T\,\vec{\mathbf{j}}$, whose explicit expression is given by (cf. [8])

$$\left(T^*T\,\vec{\mathbf{j}}\right)_{\lambda,\ell} = \sum_{\mu\in\mathbf{\Lambda}} \sum_{m=1}^{3} \left(\sum_{l=1}^{N} (A_{\ell,l}\psi_\lambda)(A_{m,l}\psi_\mu) \right) j_\mu^m, \qquad \lambda \in \mathbf{\Lambda}, \quad \ell = 1, 2, 3, \tag{17}$$

where the operator $A_{\ell,l} : L_2(V_0; \mathbf{R}) \to \mathbf{R}$ is defined as

$$A_{\ell,l}\, f := \frac{\mu_0}{4\pi} \int_{V_0} \left(\frac{\vec{\mathbf{e}}_z(\vec{\mathbf{q}}_l) \times (\vec{\mathbf{q}}_l - \vec{\mathbf{r}}\,')}{|\vec{\mathbf{q}}_l - \vec{\mathbf{r}}\,'|^3} \right)_\ell f(\vec{\mathbf{r}}\,')\, d\vec{\mathbf{r}}\,'. \tag{18}$$

Let $\mathcal{M}$ be the matrix whose entries are the coordinates of T^*T in the multiscale basis $(\psi_\lambda)_{\lambda\in\mathbf{\Lambda}}$, i.e.

$$\mathcal{M}_{(\lambda,\ell),(\mu,m)} := \sum_{l=1}^{N} (A_{\ell,l}\psi_\lambda)(A_{m,l}\psi_\mu), \qquad \lambda, \mu \in \mathbf{\Lambda}, \quad \ell, m = 1, 2, 3. \tag{19}$$

From (17) it follows

$$\left(T^*T\,\vec{\mathbf{j}}\right)_{\lambda,\ell} = \sum_{\mu\in\mathbf{\Lambda}}\sum_{m=1}^{3} j_\mu^m\,\mathcal{M}_{(\lambda,\ell),(\mu,m)}, \qquad \lambda\in\mathbf{\Lambda}, \quad \ell=1,2,3. \tag{20}$$

Since $\mathcal{M}$ is a bi-infinite matrix, in order to implement an efficient procedure to compute $T^*T\,\vec{\mathbf{j}}^{(k)}$ we need the amplitude of the entries of $\mathcal{M}$ to decay fast when λ and μ increase. Let us choose as multiscale basis a compactly supported wavelet basis with $\Omega_\lambda := \mathrm{supp}\,(\psi_\lambda) \sim 2^{-|\lambda|}$, where $|\lambda|$ denote the spatial resolution scale of ψ_λ. Moreover, we assume that the basis functions have d vanishing moments, a prescribed smoothness, and fast decay, i.e. $|\psi_\lambda| \le C2^{3/2|\lambda|}$. It can be shown that $\mathcal{M}$ has compressibility properties w.r.t. such a basis (cf. [8]), so that $T^*T\,\vec{\mathbf{j}}^{(k)}$ can be evaluated efficiently.

5 Numerical Tests

Under the assumption that the magnetometers are very close to the skull, the MEG setting reduces to a bidimensional problem in which the current flows in a plane and the magnetic field is measured by a magnetometer array located at a given height. Although in this case the inverse problem has a unique solution, it can be ill-conditioned for the presence of high noise.

In the numerical tests the brain activity is modeled by a horizontal bidimensional current dipole located in the plane $\Pi_0 = \{x, y \in \mathbf{R}, z = 0\}$ and the magnetic field is sampled by 400 magnetometers located on a regular horizontal grid at height $\delta = 1$, see Fig. 1. Note that we use adimensional measure units in the tests.

We choose as a multiscale basis the Daubechies orthonormal wavelets with $d = 4$ vanishing moments and discretize the plane Π_0 with 32 pixels for each dimension. Finally, 2 multiscale levels are used for the current decomposition. At each multiscale level, the thresholding parameter $(\rho_\lambda)_{\lambda\in\mathbf{\Lambda}}$ is chosen equal to τ times the mean of the wavelet coefficients $\vec{\mathbf{j}}^{(1)}$.

In Fig. 2 the current distribution reconstructed after 100 iterations of Algorithm `JS` is shown with $\tau = 1$. As for the other parameters, we have set $\theta_\lambda = 10^{-4}$ and $\omega_\lambda = 0$ for each $\lambda \in \Lambda$. In the figure, the current image obtained by joint-thresholding, i.e. Algorithm JS with $p = 2$ and $R > 0$, (left) is compared with the current image obtained by uncoupled soft-thresholding, i.e. Algorithm JS with $p = 1$ and $R = 0$, (right).

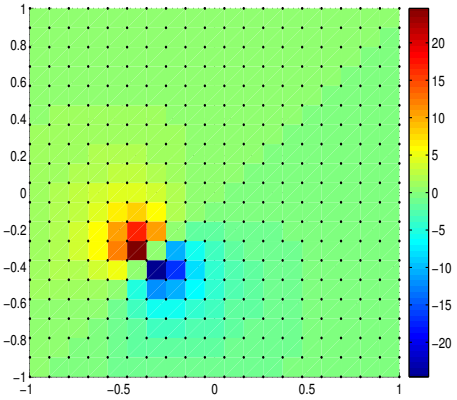

Figure 1: The magnetic field produced by a current dipole located in (-0.4,-0.4,0). The black points represent the magnetometer sites.

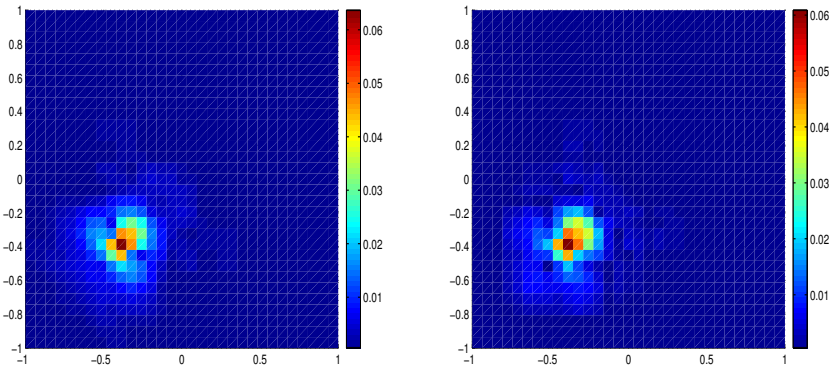

Figure 2: The current intensity reconstructed starting from the magnetic field displayed in Fig. 1 by using joint-thresholding (left) and uncoupled soft-thresholding (right).

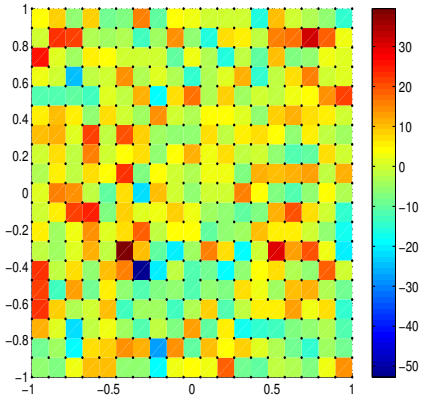

Figure 3: The noisy magnetic field produced by a current dipole located in (-0.4,-0.4,0). The magnetometer distribution is represented by black points.

In Fig. 4 the current distribution reconstructed after 100 iterations of Algorithm JS is displayed for $\tau = 20$ when high white Gaussian noise with linear signal to noise ratio equal to 0.1 is added to the magnetic field (see Fig. 3).

In case of measurements with high noise, Tikhonov regularization is not able to give an accurate current image: when the regularization parameter is chosen equal to 0 the current is not reconstructed at all (see Fig. 5, left), while a regularization parameter greater than 0 gives a blurred image (see Fig. 5, right, where the regularization parameter is chosen by means of the discrepancy principle and is equal to 356).

The ℓ_1-norm

$$\|(\vec{\mathbf{j}}_\lambda)_{\lambda\in\Lambda}\|_{\ell_1} := \sum_{\lambda\in\mathbf{\Lambda}} \|\vec{\mathbf{j}}_\lambda\|_{\mathbf{R}^2} \tag{21}$$

as a function of the thresholding parameter τ is displayed in Fig. 6 for noiseless and noisy data.

The numerical tests show that the proposed algorithm outperforms both Tichonov regularization and uncoupled iterative thresholding, especially in case of high noise.

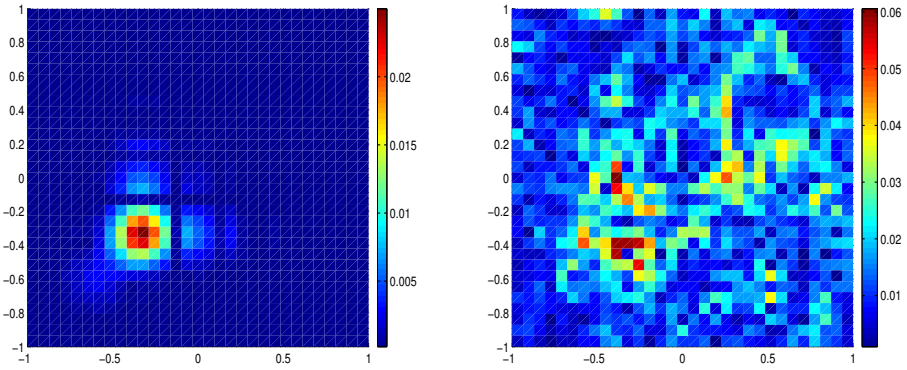

Figure 4: The current intensity reconstructed starting from the magnetic field displayed in Fig. 3 by using joint-thresholding (left) and uncoupled soft-thresholding (right).

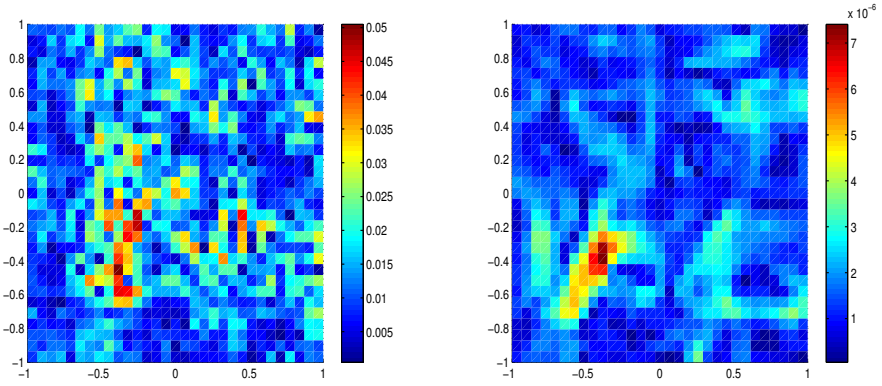

Figure 5: The current distribution reconstructed by using the Tikhonov regularization starting from the noisy magnetic field displayed in Fig. 3. Two different values of the regularization parameter have been used: 0 (right) and 356 (right).

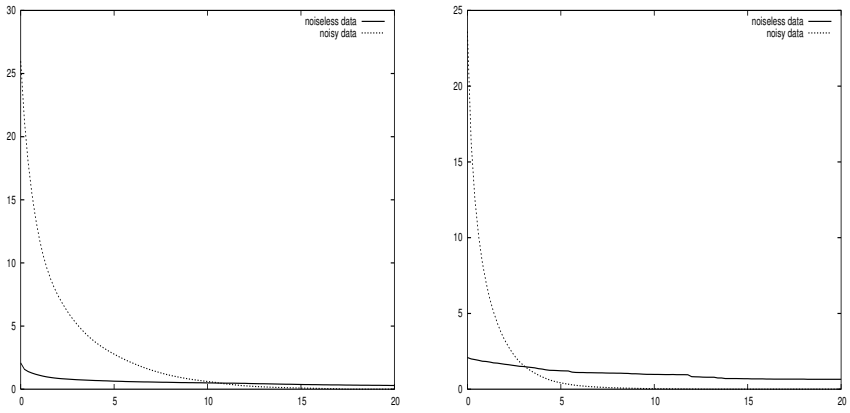

Figure 6: The ℓ_1-norm of the reconstructed current as a function of the thresholding parameter τ. The left graph refers to the joint-thresholding case while the right one refers to soft-thresholding.

References

[1] O. Christensen, *An Introduction to Frames and Riesz Bases*, Birkhäuser, 2003.

[2] I. Daubechies, Ten Lectures on Wavelets, *SIAM*, 1992.

[3] I. Daubechies, M. Defrise & C. De Mol, An iterative thresholding algorithm for linear inverse problems with a sparsity constraint, *Comm. Pure Appl. Math.* **57** (2004), 1413–1457.

[4] C. Del Gratta, V. Pizzella, F. Tecchio & L. Romani, Magnetoencephalography - a noninvasive brain imaging method with 1 ms time resolution, *Rep. Prog. Phys.* **64**, (2001), 1759-1814.

[5] D.L. Donoho, Superresolution via Sparsity Constraints, *SIAM J. Math. Anal.* **23** (1992), 1309–1331.

[6] D.L. Donoho, De-noising by soft-thresholding, *IEEE Trans. Inform. Theory* **41** (1995), 613–627.

[7] H.W. Engl, M. Hanke & A. Neubauer, *Regularization of inverse problems*, Kluwer, Dordrecht, 2000.

[8] M. Fornasier & F. Pitolli, Adaptive iterative thresholding algorithms for magnetoencephalography (MEG), *J. Comput. Appl. Math.*, **221**, 2008, 386-395.

[9] M. Fornasier & H. Rauhut, Recovery algorithms for vector valued data with joint sparsity constraints, *SIAM J. Numer. Anal.*, **46**, 2008, 577-613.

[10] M. Fornasier & H. Rauhut, Iterative thresholding algorithms, *Appl. Comput. Harmon. Anal.*, **25**, 2008, 187-200.

[11] R. Kress, L. Kühn & R. Potthast, Reconstruction of a current distribution from its magnetic field, *Inverse Problem 18* (2002), 1127–1146.

[12] J. Sarvas, Basic mathematical and electromagnetic concepts of the biomagnetic inverse problem, *Phys. Med. Biol. 32* (1987), 11–22.